A novel coupling control with decision-maker and PID controller for minimizing heating energy consumption and ensuring indoor environmental quality

Yang Wang[a,b,1], Jens M. Kuckelkorn[c], Daoliang Li[a], Jiangtao Du[d]

a) College of Information and Electrical Engineering, China Agricultural University, 100083, Beijing, P. R. China

b) School of the Built Environment and Architecture, London South Bank University, SE1 0AA, UK

c) Division of Technology for Energy Systems and Renewable Energy, Bavarian Center for Applied Energy Research (ZAE Bayern), 85748, Garching, Germany

d) School of the Built Environment, Liverpool John Moores University, Liverpool, UK

[1] Author to whom correspondence should be addressed.
Address: College of Information and Electrical Engineering, China Agricultural University, Beijing, China
Contact: wanghongyang1767@gmail.com, wangy47@lsbu.ac.uk (**Yang Wang**);

Abstract

Due to climate change, global energy crisis and high-quality life requirement for people, decreasing building energy consumption and enhancing indoor environment quality through control of heating, ventilation and air conditioning systems tend to be increasingly important. Therefore, favorable control methods for heating and ventilation systems are urgently necessary. In this work, a new coupling control with decision-maker was proposed, developed and investigated; meanwhile, several demand controlled ventilation strategies combined with heating control method was compared considering heating energy consumption, thermal comfort and indoor air quality. In order to properly model the service systems, the air change rates and thermal time constants have been first measured in a reference office installed with commonly applied bottom-hinged tilted windows in our low-energy building supplied by geothermal district heating. Then, simulations have been carried out across two typical winter days in the reference office. The results illustrate that the proposed combination of suitable heating and DCV coupling control methods with decision-maker and PID controller could greatly reduce heating consumption in the reference room during the office time: around 52.4% (4.4 kWh energy saving) per day in winter in comparison to a commonly suggested method of intensive and brief airing. At the same time, it could ensure indoor CO_2 concentration to keep within the preset ranges (Pettenkofer limit: 1000 ppm) as well as low variations of indoor temperature (STD: 0.1 ^{o}C).

Keywords and Main body

Keywords

Coupling Control with Decision-maker; Heating System; PID Control; Demand Controlled Ventilation (DCV); Heating Consumption; Pettenkofer Limit

Main body

1 . Introduction

Buildings in Germany are responsible for around 40% of total annual energy consumption [1-3] and one third of CO_2 emissions into the atmosphere, which could result in climate changes due to the depletion of ozone layer [4-6]. In addition, above 70% of building energy in Germany is consumed by the space heating [4]. Similar statistical results occur in the major of other countries, where around 40% of total annual energy has been consumed in buildings [1, 7]. Demand Controlled Ventilation (DCV) could be used to reduce heating consumption while maintaining an acceptable indoor environment [8]. Over the last few decades, a number of studies on the applications of DCV have been completed, and therefore be classified as: case studies via tests on site [9-10], topology control and control strategy analysis [11-12], selection of diverse controlled parameters of indoor air flow adjustments [13-14].

Indoor air quality (IAQ) is a crucial parameter to evaluate ventilated room/building performance and indicate potential impacts on occupant health. IAQ could be influenced by diverse gaseous components (including VOCs, particulate matters, NO_x,

Ozone, CO_2, formaldehyde). CO_2 is the major indoor contaminant generated by occupants through respiration [15-16]. The concentration of CO_2 is therefore employed as an IAQ indicator in this article. During the past decades, a number of studies have investigated the CO_2-based DCV [9, 17-27]. Pettenkofer limit of 1000 ppm for CO_2 concentration [19] has been regarded as IAQ indicator and standard, particularly in learning and teaching environments [18, 20]. Behravan et al. [21] proposed a CO_2 DCV approach with Matlab/Simulink used in developing HVAC systems of building automation management systems, focusing on faults diagnosis and detection. Fan et al. [17] designed and optimized a CO_2-DCV in a typical Japanese office. The measured data showed that with the application of energy recovery ventilation system for DCV, the energy consumption can be decreased by 20-30%. Nassif [22] proposed a novel CO_2-based DCV method used for the HVAC system of multi-zone. This proposed DCV strategy could achieve energy saving up to 23%. Using limited sensors in multi-zones, moreover, Shan et al. [23] introduced a new DCV strategy that has similar performance to a full-sensor system. This DCV strategy could achieve significant energy saving (around 50%) and at the same time maintain acceptable IAQ. Lu et al. [24] proposed another CO_2-based DCV strategy in sports training arenas. Around 34% of energy from ventilation could be saved in comparison to proportional controller; in addition, indoor air CO_2 concentration could be controlled within set-point for every training section. Ng et al. [25] investigated the CO_2-based DCV based on the ASHRAE Standard 62.1-2010, and found that DCV for ASHRAE 62 results in mostly lower ventilation rate than

ASHRAE 62.1. Merzkirch et al. [26] tested 3 different DCV solutions on site. Then, a novel semi-centralized valve-less solution in residential buildings has been proposed. The monitored results illustrated primary energy saving of approximately 50% without compromising IAQ. Ahmed et al. [27] studied building energy performance and indoor climate in Finnish low-energy building using chilled beams via controlled flow rate. The proposed DCV system could save 7-8% of primary energy in comparison with constant air volume (CAV) unit based on controlled operation approach. Hesaraki et al. studied the DCV in new domestic buildings [28]. In the proposed system, the heating demand of electricity and the ventilation consumption of ventilating fan have been reduced by 30% and 20% respectively.

Apart from the CO_2-based DCV studies, control strategies or controllers for DCV have been also investigated recently. Zucker et al. [29] employed the variable air volume (VAV) controllers to provide a defined volume flow to each zone. A linear controller was developed to control the ventilation system. The results showed the new approach can achieve higher efficiency of ventilation system operation, and would also keep indoor comfort and reduce the installation costs. Sun et al. used a pressure-independent VAV control for managing indoor temperature [30]. Thomas et al. studied and compared CAV controller and VAV controller respectively, for the ventilation air volume flow in commercial buildings [31]. Ng et al. [25] proved that the proportional control method is more acceptable than occupancy detecting method in an individual-zone unit. Ahmed et al. applied PI controller to control the room temperature

via regulating the cooling coil mass flow [27]. Vaccarini et al. [32] proposed a model predictive control algorithm of ventilation for underground stations of Barcelona. Over 30% of energy saving in ventilation unit has been obtained, with the pre-existing comfort levels. Kaam et al. [33] developed the VAV control systems used in time-averaged ventilation, which can adjust every zone VAV damper at the starting and ending stages.

The studies aforementioned were focusing on either IAQ or building energy efficiency or both of them, through adopting the DCV system with CAV or VAV controller, and the control strategies including traditional control such as linear control, proportional control and advanced control (e.g. MPC). However, two significant aspects have not been properly investigated in the area of ventilation systems and relevant controls, especially with the increasing requirements of comfortable and healthy indoor climates in school buildings. First, the possibility to apply natural ventilation using a controllable and smart approach in the environment mentioned above could still be a challenge, due to the fact that it is very hard to balance between IAQ and indoor comfort. Second, indoor comfort and IAQ are increasingly considered as a priority for the indoor ventilations system design, which is always changing the system design and controls based on energy efficiency. Clearly, it is necessary to seek the new and easy-realizing methods for DCV combining with heating system to maintain IEQ, and at the same time minimize heating energy consumption and CO_2 equivalent emissions in buildings.

A coupling control combining DCV and heating system was preliminarily reported in a conference article [34]. In this work, this method was improved using a decision-maker and was further tested in a reference office room of school building, aiming to try to fill in the research gap mentioned above. The objective is to compare various ventilation control strategies and methods with decision-maker through statistical techniques, and to develop and design a novel and easy-realizing PID controlled method with very tiny window opening angle, which can not only minimize heating energy consumption and CO_2 equivalent emissions, also ensure IAQ and acceptable thermal comfort. In the following parts, a reference office room inside one low energy building is firstly presented and modelled. Then, the thermal time constants and air exchange rates measured in the room are explained and applied to validate the numerical simulations. Finally, a case study for new coupling control with decision-maker will be demonstrated through comparing several different DCV methods.

2. Physical model description

The study was conducted in a new-built low-energy public school building located in area of Erding, Munich (see Fig. 1). It adopted a geothermal district heating system. Heat transfer coefficients of the envelopes are lower, including exterior wall 0.128 W/m^{2}K, ceiling 0.095 W/m^{2}K, floor 2.45 W/m^{2}K and window 0.870 W/m^{2}K. The solar heat gain coefficient of window is 0.5.

A reference office room (see Fig.1(b)) in the building installed with extensive measurement and control systems has been modelled using the building energy simulation (BES) software package. Its dimensions are 6.5 m (length) × 5 m (width) × 3 m (height). There are two windows with the size of 1.7 m × 2.1 m and 1.0 m × 1.9 m, respectively, both of which are normal tilted bottom-hinged windows having a maximal opening angle of 4^o. The opening factor is defined as follows,

$OF = \alpha/90^o$ (1)

where α is an angle of opening or tilting window. OF = 0 indicates that window is off completely, OF = 0.04 denotes its maximal opening angle is 4^o, and OF = 1 means that an opening angle is 90^o, which means intensive and brief airing.

The maximal inlet water temperature of radiator heating supplied by the hot water boiler from the geothermal district heating in Erding is 45 ^{o}C, the maximum supply hot water flow rate is 3.5 m^3/h. Fig.2 shows the schematic diagram of that reference office with combination of DCV control and radiator heating systems.

3. Measurement of thermal time constant and air change rate

Thermal time constants measurements

Thermal time constant is the time requested for a thermistance to change 63.2% of the whole difference between the initial temperature and final temperature due to one step function change in temperature [35]. Based on the thermal time constant definition, an exponential decay model with τ as the thermal time constant is used,

$$T = T_0 + ae^{\frac{-t}{\tau}} \qquad (2)$$

Where T is the indoor temperature measured in ^{o}C, T_0 is the indoor temperature in balance for the measurement in ^{o}C, a is the beginning and ending temperature difference for balance during the measurement in ^{o}C, t is the measurement time in minute, τ is thermal time constant in minute. According to measurement data for the reference office room and the abovementioned model, ideal fitting decay equations for decreasing ($T_{dec.}$) and increasing ($T_{inc.}$) temperatures due to switching on and off the radiator heating, respectively, (see Fig. 3) were determined and shown as follows:

$T_{dec.} = 22.35 + 1.92e^{\frac{-}{150.58}}$ (R_{sqr} is 0.993) (3)

$T_{inc.} = 24.15 - 1.391e^{\frac{-}{157.48}}$ (R_{sqr} is 0.972) (4)

where R_{sqr} means how well the regression lines fit measurement data. The closer R_{sqr} value is to 1, the better an ability of the model predicts the regression trend. Therefore, two of above regression equations are used in measuring the thermal constant. Table 1 illustrates the Standard Deviation (STD) errors for factors of the abovementioned models. Table 1 shows both thermal constant STD errors are expectedly approaching 0, which means thermal time constants approximate real time constants for the measurement data. According to Eqs. (3) and (4), thermal time constants of the reference office room have been calculated and known to be 2.5 hours (151 min) for reducing temperature and 2.6 hours (157 min) with regard to rising temperature. Fig. 3 illustrates measuring data for room temperatures, the steps of temperature are mostly because of resolution of digital sensors. Because of heating energy storage within the envelopes, i.e., effect of thermal mass results in thermal inertia over indoor temperature

variations, two similar thermal constants appear. The aforementioned values of thermal time constants are employed for the following simulations.

Air exchange rates measurement

Air leaks is often considered as one of major reasons of building heating or cooling loss. The performance of air tightness was measured in earlier field measurements via using blower door test method [36], and testing results ACH_{50} have been known to be 0.17 h^{-1} and 0.13 h^{-1} [4]. The air exchange each hour for the building pressure at 50 Pa can be defined as follows,

$ACH_{50} = Q_{50}/V$ (5)

where ACH_{50} is air exchange at 50 Pascal in h^{-1}, Q_{50} is air flow rate in m^3/h, V is a tested building or room volume in m^3. Thus, the infiltration rate could be also determined by $ACH_{50}/20 = 0.01$ 1/h [36, 37].

4. Validation of BES models

TRNSYS/TRNFlow (Transient System Simulation), the BES programme used in this stud, was developed based on the network model [38, 39]. The programme can dynamically identify the significant parameters for building energy performance and thermal environment, e.g. calculation of energy demand for heating and cooling, evaluation of thermal comfort etc. The thermal model of TRNSYS includes convective heat flux to the air node, and the heat conduction at the wall surface equations [38]. TRNFlow integrates the multi-zone air flow model COMIS into the thermal multi-zone building model type 56 [39], which could simulate the air flows between zones and

natural ventilation systems.

Even though TRNSYS/TRNFlow has been previously applied in several studies [40-43], it is still necessary to validate it before employing it as a simulation tool in this study. A validation has been completed via comparing simulation results against measured data in the reference room (Fig.1(b)). First, a Thermoken surface mounting sensor has been used to measure the indoor air temperature, with an accuracy of $\pm 0.5\ ^{o}C$ and a measurement range ($+5\ ^{o}C \sim +45\ ^{o}C$). The temperature measurement in the room has been implemented on Jan. 5th 2015, taking into account only the envelop infiltration. In Fig. 4(a), it can be clearly found that the measured indoor temperature and BES simulated results can achieve a proper agreement with each other. The maximum difference between simulations and measured data is only around 0.4 ^{o}C, which expressed the validation of temperature simulation and can ensure the reliability of the succeeding simulation investigations. Second, an AERASGARD CO_2 sensor having an accuracy of ± 100 ppm was installed at the top half of the wall far from the openings in the room, which has been recommended as the typical location for installing single CO_2 sensor [15-16]. The measurement of indoor CO_2 concentration in the reference room with 30 occupants and ventilation rate of 3.7 1/h has been performed on Nov. 20, 2014. During the measurement, the outside air CO_2 level is 390 ppm, while mean wind speed and direction are 0.45 m/s and 270.4^{o} respectively. In Fig. 4(b), it could be observed that measured indoor CO_2 concentration and BES TRNFlow simulations are very similar. The maximum discrepancy between measurements and

simulations is around 80 ppm. This result again enhanced the reliability of BES program and the following simulation investigation. Third, the comparisons of indoor temperatures between measurements and simulations are given in Fig. 4(c), based on the date of Nov 20, 2014 (corresponding to indoor CO_2 concentration measurement in Fig. 4(b)). It can be apparently found that the simulated data well agree with the measurements.

In addition, the validation of building system modelling using TRNSYS/ TRNFlow including thermal (temperature) and air-flow (CO_2) models has been conducted using several types of monitored data across a 3-year evaluation phase from our database MedVIEW 2 [4, 41].

These validation activities above can well support the application of TRNSYS/TRNFlow in this study.

5. Coupling control for ventilation and heating systems

Ventilation methods

There are several different types of ventilation approaches including manual ventilation and DCV method, which have been investigated by lots of researchers [11-14].

I) Manual control: the kind of method means normal recommendation: intensive and brief airing via completely opening windows with a brief duration e.g. approximately 5 minutes frequently each 1 to 2 hours.

II) ON/OFF control (Bang-bang control): the DCV employs the measuring

indoor CO_2 concentration so as to 1) open windows for a given duration e.g. 1 minute for OF = 1 or 5 minutes for OF = 0.04 over pre-set upper threshold, i.e., *set-point* in ppm is exceeded or 2) On and off windows based on pre-set upper, i.e., $set\text{-}point_{max}$ in ppm and lower, i.e., $set\text{-}point_{min}$ in ppm CO_2 concentration threshold levels. The opening has been set in BES with OF variable defined previously below,

$$OF(t) = Ge(CO_2\%(t), Setpoint) \text{ x } OF_{max} \quad (6)$$

where *Ge* is a Boolean operator: greater or equal, it will return one if 1st expression of brackets is greater than or equals 2nd one; it will return 0 otherwise. $CO_2\%(t)$ is the measured CO_2 concentration, OF_{max} is the maximal opening factor. There are two values 1 and 0.04 investigated in this work; the BES results with the value of one are in comparison with manual control situation; 0.04 means complete opening angle.

III) PID control: this type of DCV method is still according to the measured indoor CO_2 concentration, however, permits for the successive OF value rather than just its opening binary state (on/off) as employed in the following Eq. (7). The PID control equation is

$$y = K_p \left[e(t) + \frac{1}{T_i} \int_0^t e(\tau) d\tau + T_d \frac{d}{dt} e(t) \right] \quad (7)$$

Where y is the controller output, K_p is proportional gain of the controller gain, e is the error value defined as the difference between the real CO_2 concentration and its set point, T_i is the integral time, T_d means the derivative

time. PID controller tries to minimize the error via adjusting the process control variable which is OF here (and for the radiator heating system: the inlet temperature and water flow rate) via its output y. In this study, controller parameters K_p, T_i and T_d have been determined in term of the general guidelines of the Ziegler-Nichols adjusting method [44]. T_d was fixed to zero in order to avoid the overshoot, i.e., higher CO_2 concentration as its set-point level, causing a PI controller.

Heating methods

I) Manual control: the approach means the regular recommendation, i.e., switch on the radiator heating manually for a period of time when required.

II) ON/OFF control (Bang-bang control): the DCV employs the measuring temperature so as to turn on radiator heating with regard to a given duration until it meets the set-point value 21 ^{o}C when occupied. Otherwise, the radiator heating will be switched off automatically by the controller.

III) PID control: In this work, the PID controller based radiator heating has three non-zero factors. The indoor set-point temperature is 21 ^{o}C during the work hours starting at 8 am until 6 pm during working days.

Development of coupling control strategy with a Decision-maker

According to the aforementioned ventilation and heating control methods, a coupling control strategy with Decision-maker has been developed. Fig. 5 illustrates the schematic diagram of the control systems with Decision-maker for coupling DCV and

radiator heating system in the reference office room. Seen from the Fig. 5, one Decision-maker could judge the indoor conditions based on the real-time feedback of CO_2 concentration sensor and indoor air temperature sensor, it will determine if it need trigger DCV and heating systems and how to adjust controller parameters of DCV and heating. Table 2 shows the diverse combinations of coupling control methods with Decision-maker for ventilation and heating systems. There are six different types considering indoor real-time conditions and period of time. Typical case studies will be carried out in the subsequent simulation section.

6. Results and discussion

There are some assumptions in this work: 1) two occupants working in the reference office between 8 am and 6 pm from Monday to Friday; 2) relative humidity for indoor air is 50%. One occupant for sitting situation could produce around twenty litres' pure CO_2 each hour because of respiration; human being is the heating source of a power with around 100 W, which is the total heat gain [45]. Taking into account the volume V = 97.5 m^3 (6.5 x 5 x 3 m^3) of the reference office room, the indoor CO_2 concentration 1000 ppm will be reached over around one and half hours when there was without air change completely when outside CO_2 concentration is 390 ppm. The setting point CO_2 concentration levels within 750 ppm and 1500 ppm have been studied for this work. For the case of closed window, the infiltration is not considered in the air flow model; whilst in the case of opening window, the infiltration rate with 0.01 1/h will be considered. The simulation time step is 1 minute in the following numerical

investigation.

Considering indoor temperature, an average level of 21 ^{o}C has been selected as the set-point during working time. The indoor temperature for night, i.e., vacant situation, for working days is fixed at 19 ^{o}C so as to save energy (comparing with 21 ^{o}C during whole day/night for working days, the decrease of 4.8% could be reached using PID controller for one common winter day) and improve the heating efficiency for the next working day.

In this work, weather condition including outdoor temperature, relative humidity and wind speed and direction of 2 representative winter days monitored and recorded via our weather condition Medview2 database [4] of low-energy school building during the last 7 years: 1) foggy, not very cold under small variations within +0.21 ^{o}C and +1.12 ^{o}C; 2) clear skies, obvious temperature gaps between day and night with around 20 ^{o}C (-15.0 ^{o}C to +4.0 ^{o}C). Other different set-point combinations including (22/19) ^{o}C and (21/18) ^{o}C have been also investigated due to comparison. Because the temperature of lower setback, e.g. under temperature of dew point, during night might result in water condensation, mold growth and an unbearable low indoor temperature, even the large improving temperature stage via switching on the heating in early morning next day. It is interesting to note for the above alternative temperature set-points: compared with the combination (21/19) ^{o}C, the energy consumption improves by around 4% while utilizing (22/19) ^{o}C, however, it will be reduced by 2.7% for the case of (21/18) ^{o}C, which was simulated using PID controller for the representative winter day one. The temperature

and human effects on CO_2 concentration indoors have been investigated [47] and are not obvious e.g. indoor CO_2 concentration just decreases from 1060 ppm to 986 ppm with the increasing of indoor temperature from 10 ^oC to 20 ^oC when natural ventilation rate is kept as 3.7 1/h. In this work, it mainly focuses on the comparison of different DCV methods based on CO_2 concentration set points and presents a novel coupling control with decision-maker and PID controller.

With regard to the aforementioned coupling control strategy with decision-maker, type No. 5 was chosen as a case study in this work, which is also a main scenario for the reference office room. Figs. 6 to 8 illustrate the indoor temperature T_{in} and outdoor temperature T_{out} as well as indoor air CO_2 concentrations considering diverse ventilation approaches mentioned earlier. Both officers get to room at 8 am, both of them then start exhaling CO_2, CO_2 concentration achieves the set-point 1000 ppm (i.e. Pettenkofer limit) at 10:10 am. For ON/OFF (Bang/bang) control in Figs. 6 and 7, OF turns into instantly OF_{max} and the window(s) are completely opened. For the case of OF =1 (manual control), i.e., intensive and brief airing. Room temperature changing, which will influence thermal comfort, is smaller around 2 ^oC for the case of OF = 0.04 in comparison with the case of OF = 1. Pettenkofer limit 1000 ppm is not surpassed; average indoor CO_2 concentration is virtually identical to both methods.

For the purpose of comparing ventilation control approaches and the potential to shrink energy consumption when maintaining high IAQ and thermal comfort, several different simulations demonstrated in Figs. 6, 7 and 8 have been carried out. Table 3 and

4 illustrate the results in which average values (AVE), standard deviation (STD) of room temperature, and CO_2 concentration demonstrate diverse control approaches level. It is noticed radiator is the heating with a relatively big thermal time constant illustrated in Section 3, it has thus relatively big temperature control inertia and room temperature could not be varied as quickly as an air conditioning or convector heater.

Table 3 illustrates the simulation results for diverse scenarios including without any air change, and just infiltration, i.e., both of windows turned off, as well as infiltration plus diverse ventilation approaches. With the aim of directly comparing the values for Q_{hair}, which is the heating energy required to heat the room and the colder outdoor airflow via windows, average values of T_{in} and CO_2% for all ventilation approaches have to be identical. But, it is noticed that T_{in} and CO_2% couple and affect each other, complicating simultaneous controlling of two factors. For Table 4, values of Q_{tran} (i.e., heating loss because of heat transmission between indoor and outdoor via façade), Q_{hair}, Q_{inf} (i.e. thermal energy because of infiltration) have been listed with regard to 2 representative winter days.

Seen from Table 3, Q_{hair} because of the common suggested intensive and brief airing (each two hours around five minutes: type 3) is around two times in comparison with that best strategy (i.e., PID controller under tiny openings; 860 ppm), which could save around three kWh for thermal energy each day and maintain indoor temperature variations extremely small (i.e., its STD is just 0.1 ^{o}C), which conversely maximizes thermal comfort. While Pettenkofer limit of 1000 ppm has been selected, it could save

heating energy 4.4 kWh each day.

Observed from Tables 3 and 4, it could be concluded the entire shrinking of heating energy Q_{hair} required to heat the office during working time from 8 am to 6 pm (require for ventilation) for approximately 52.4% could be reached ((8.4 kWh – 4.0 kWh)/8.4 kWh = 0.524). With regard to the 2nd representative winter day as mentioned from initial part of Section 6, the abovementioned heating saving improves up to 5.5 kWh (see Table 4). Because of the higher heating consumption Q_{hair} for this case, the reduction remains 51.4% almost same ((10.7 kWh – 5.2 kWh)/10.7 kWh = 0.514).

The CO_2 equivalent emissions resulted from heating consumption have been also investigated according to CO_2 equivalent factor 0.177 kg/kWh of district heating in Germany [46]. Fig. 9 illustrates CO_2 equivalent emissions for nine types of DCV corresponding to Q_{air} in Table 3. Seen from Fig. 9, the CO_2 equivalent emissions will be reduced by 2.2656 kg (2.9736 kg – 0.708 kg) per typical winter day using the the PI(D)-based coupling control of DCV strategy and heating system (type 9) in comparison with that usually commended intensive and brief airing approach (type 4).

Fig. 10 shows the comparisons between diverse set points for CO_2 concentration among 750 ppm until 1500 ppm while PID controller has been employed. Observed from Fig. 10, when its setting point decays from 1000 ppm to 750 ppm, Q_{hair} rises by around 90% ((7.5 kWh – 4.0 kWh)/4.0 kWh = 0.875) . However, with regard to 1500 ppm, Q_{hair} reduces by around 40% ((4 kWh - 2.5 kWh)/4 kWh = 0.375) compared with the set point 1000 ppm.

7. Conclusions

In this work, a new coupling control with Decision-maker has been investigated and developed through a typical case study using statistical techniques, which combines the DCV and indoor temperature control strategies for the purpose of reaching high IAQ and thermal comfort however maintaining minimal heating energy consumption. CO_2 concentration has been employed as an indicator of IAQ. Diverse ventilation methods have been contrasted and evaluated with BES and are according to one reference office model considering its real parameters via measurements in our low-energy building.

The BES results from Table 3 illustrate that, compared with the usually commended intensive and brief airing approach, PID-based demand controlled ventilation method with the quite tiny opening angle, which is presented via an OF factor, could completely maintain IAQ with an expected scope and decrease thermal energy with regard to that office among the working time (when ventilation is necessary) by around 4.4 kWh regarding one typical winter day in Munich for a foggy condition, by about 5.5 kWh for another typical day whose temperatures ranged from -15.0 ^{o}C to 4.0 ^{o}C. CO_2 equivalent emissions will be reduced by 2.27 kg per typical winter day using PID-based coupling control of DCV method and radiator heating system compared with the usually commended intensive and airing approach. Meanwhile, one proposed DCV method under quite tiny opening factor could ensure extremely tiny indoor temperature fluctuations (STD is 0.1 ^{o}C), which could maximize the thermal comfort.

Heating consumption Q_{hair} is obviously higher regarding small CO_2 setting point levels: with regards to PID-based DCV approach under quite tiny opening and for Pettenkofer limit 1000 ppm, Q_{hair} has to increase by around 90% (3.5 kWh) for 750 ppm, and could decrease by approximately 40% (1.5 kWh) for the case of 1500 ppm.

This research can benefit for those coupling DCV and heating control systems design and optimization for those low-energy buildings with winter conditions. Further detailed researches, concerning more variations of actual RH for indoor air and complex RH model, the impacts of human beings and their behavior on RH/enthalpy, development of renewable energy and energy storage technologies how to embed in and combine with current low-energy building favorably etc., will be conducted.

Acknowledgments

This research was financially supported by the German Federal Environmental Foundation (Deutsche Bundesstiftung Umwelt, DBU AZ 26170/02-25 & 35), China Agricultural University Excellent Talents Plan, and Fundamental Research Funds for the Central Universities in China (Grant No. 2018QC174). The authors are very grateful to the reviewers who provided with constructive and useful comments.

References

[1] D. Liu, F. Y. Zhao, G. F. Tang. Active low-grade energy recovery potential for building energy conservation. Renewable and Sustainable Energy Reviews 14 (2010)

2736-2747.

[2] Y. Wang, J. Kuckelkorn, F. Y. Zhao, H. Spliethoff, W. Lang. A state of art of review on interactions between energy performance and indoor environment quality in Passive House buildings. Renewable and Sustainable Energy Reviews 72 (2017) 1303-1319.

[3] S. Schimschar, K. Block, T. Boermans, A. Hermelink. Germany's path towards nearly zero-energy buildings – enabling the greenhouse gas mitigation potential in the building stock. Energy Policy 39 (2011) 3346-3360.

[4] Y. Wang. *Optimization for building control systems of a school building in Passive House Standard*. PhD Dissertation, Media Technical University of Munich, Munich, 2015.

[5] N. Bakar, M. Hassan, H. Abdullah etc. Energy efficiency index as an indicator for measuring building energy performance: A review. Renewable and Sustainable Energy Reviews 44 (2015) 1-11.

[6] A. Gonzalez, J. Diaz, A. Caamano, M. Wilby. Towards a universal energy efficiency index for buildings. Energy and Buildings 43(4) (2011) 980-98 .

[ ] M. Gustafsson, G. Dermentzis, J. A. Myhren, C. Bales, F. Ochs, S. Holmberg, W. Feist. Energy performance comparison of three innovative HVAC systems for renovation through dynamic simulation. Energy and Buildings 82 (2014) 512-519.

[8] J. Jia, W. Lee, H. Chen, H. Li. A simplified model for evaluating the energy saving potential of adopting demand controlled ventilation in office buildings in Hong Kong. Indoor and Built Environment 0(0) (2016) 1-12.

[9] S. W. Wang, J. Burnett, H. S. Chong. Experimental validation of CO_2-based occupancy detection for demand-controlled ventilation. Indoor Built Environment 8 (1999) 377-391.

[10] C. Chao, J. S. Hu. Development of an enthalpy and carbon dioxide based demand control ventilation for indoor air quality and energy saving with neutral network control. Indoor Built Environment 13 (2004) 463-475.

[11] X. H. Xu and S. W. Wang. An adaptive demand-controlled ventilation strategy with zone temperature reset for multi-zone air-conditioning systems. Indoor Built Environment 16 (2007) 426-437.

[12] S. W. Wang, Z. W. Sun, Y. J. Sun, N. Zhu. Online optimal ventilation control of building air-conditioning systems. Indoor Built Environment 20 (2011) 129-136.

[13] C. Chao, J. S. Hu. Development of a dual-mode demand control ventilation strategy for indoor air quality control and energy saving. Building and Environment 39 (2004) 385-397.

[14] A. Afshari, N. C. Bergsoe. Humidity as a control parameter for ventilation. Indoor Built Environment 12 (2003) 215-216.

[15] Y. Wang, F. Y. Zhao, J. Kuckelkorn, etc. School building energy performance and classroom air environment implemented with the heat recovery heat pump and displacement ventilation system. Applied Energy 114 (2014) 58-68.

[16] Y. Wang, F. Y. Zhao, J. Kuckelkorn, D. Liu, L. Q. Liu, X. C. Pan. Cooling energy efficiency and classroom air environment of a school building operated by the heat

recovery air conditioning unit. Energy 64 (2014) 991-1001.

[17] Y. Fan, K. Kameishi, S. Onishi, K. Ito. Field-based study on the energy-saving effects of CO_2 demand controlled ventilation in an office with application of energy recovery ventilators. Energy and Buildings 68A (2014) 412-422.

[18] M. Bayoumi. Energy saving method for improving thermal comfort and air quality in warm humid climates using isothermal high velocity ventilation. Renewable Energy 114B (2017) 502-215.

[19] M. Von Pettenkofer. Ueber den Luftwechsel in Wohngebaeuden. Cotta, Munich, 1858.

[20] D. Norbaeck, K. Nordstroem, Z. Zhao. Carbon dioxide (CO_2) demand-controlled ventilation in university computer classrooms and possible effects on headache, fatigue and perceived indoor environment: an intervention study.

[21] A. Behravan, R. Obermaisser, A. Nasari. Thermal dynamic modeling and simulation of a heating system for a multi-zone office building equipped with demand controlled ventilation using MATLAB/Simulink. 2017 International Conference on Circuits, System and Simulation.

[22] N. Nassif. A robust CO_2-based demand-controlled ventilation control strategy for multi-zone HVAC systems. Energy and Buildings 45 (2012) 72-81.

[23] K. Shan, Y. Sun, S. Wang, C. Yan. Development and In-situ validation of a multi-zone demand-controlled ventilation strategy using a limited number of sensors. Building and Environment 57 (2012) 28-37.

[24] T. Lu, X. Lv, M. Viljanen. A novel and dynamic demand-controlled ventilation strategy for CO_2 control and energy saving in buildings. Energy and Buildings 43-9 (2011) 2499-2508.

[25] M. O. Ng, M. Qu, P. Zheng, Z. Li, Y. Hang. CO_2-based demand controlled ventilation under new ASHRAE Standard 62.1-2010: a case study for a gymnasium of an elementary school at West Lafayette, Iniana. Energy and Buildings 43-11 (2011) 3216-3225.

[26] A. Merzkirch, S. Maas, F. Scholzen, D. Waldmann. A semi-centralized, valveless and demand controlled ventilation system in comparison to other concepts in field tests. Building and Environment 93-2 (2015) 21-26.

[27] K. Ahmed, J. Kurnitski, P. Sormunen. Demand controlled ventilation indoor climate and energy performance in a high performance building with air flow rate controlled chilled beams. Energy and Buildings 109 (2015) 115-126.

[28] A. Hesaraki, S. Holmberg. Demand-controlled ventilation in new residential buildings: Consequences on indoor air quality and energy savings. Indoor and Built Environment 24-2 (2015) 162-173.

[29] G. Zucker, A. Sporr, A. G. Marijuan etc. A ventilation system based on pressure-drop and CO_2 models. Energy and Buildings 155 (2017) 378-389.

[30] Z. Sun, S. Wang, Z. Ma. In-situ implementation and validation of a CO_2-based adaptive demand-controlled ventilation strategy in a multi-zone office building. Building and Environment 46-1 (2011) 124-133.

[31] T. Thomas, J. Kotik, M. Schmoellerl etc. Energy savings through implementation of a multi-state Time Control Program (TCP) in demand-controlled ventilation of commercial buildings. Energy and Buildings 164 (2018) 33-47.

[32] M. Vaccarini, A. Giretti, L. C. Tolve, etc. Model predictive energy control of ventilation for underground stations. Energy and Buildings 116 (2016) 326-340.

[33] S. Kaam, P. Raftery, H. Cheng, G. Paliaga. Time-averaged ventilation for optimized control of variable-air-volume systems. Energy and Buildings 139 (2017) 465-475. [34] Y. Wang, Y. Shao, C. Kargel. Demand controlled ventilation strategies for high indoor air quality and low heating energy demand. Proceedings of Conference on Instrumentation and Measurement Technology (I2MTC) (2012) 870-8 5.

[35] R. W. Lewis, P. Nithiarasu, K. N. Seetharamu. Fundamentals of the finite element method for heat and fluid flow. Wiley, England, 2004.

[36] M. H. Sherman. The use of blower-door data. Indoor Air 5 (1995) 215-224.

[37] M. H. Sherman. Estimation from leakage and climate indicators. Energy and Buildings 10 (1987) 81-86.

[38] TRNSYS 17 Manual. Solar Energy Lab, University of Wisconsin-Madison, Madison, 2010.

[39] TRNFlow Manual. TRANSSOLAR Energitechnik GMBH, Version 1.3, Stuttgart, 2006.

[40] B. L. Gowreesunker, S. A. Tassou, M. Kolokotroni. Coupled TRNSYS-CFD simulations evaluating the performance of PCM plate heat exchangers in an airport

terminal building displacement conditioning system. Building and Environment 65 (2013) 132-145.

[41] Y. Wang, J. Kuckelkorn, F. Y. Zhao, D. Liu, A. Kirschbaum, J. L. Zhang. Evaluation on classroom thermal comfort and energy performance of passive school building by optimizing HVAC control systems. Building and Environment 89 (2015) 86-106.

[42] S. Firlag, S. Murray. Impact of airflows, internal heat and moisture gains on accuracy of modeling energy consumption and indoor parameters in passive building. Energy and Buildings 64 (2013), 372-383.

[43] S. Leenknegt, R. Wagemakers, W. Bosschaerts, D. Saelens. Numerical study of convection during night cooling and the implications for convection modeling in building energy simulation models. Energy and Buildings 64 (2013) 41-52.

[44] K. J. Astroem, T. Haegglund. Advanced PID Control. ISA-The Instrumentation, Systems, and Automation Society, USA, 2005.

[45] ISO EN 7730, Ergonomics of the thermal environment – analytical determination and interpretation of thermal comfort using calculation of the PMV and PPD indices and local comfort criteria, International Standards Organization, Geneva, 2005.

[46] C. Jacobsen, C. Hutter, H. P. Kirchmann, W. Wild, H. Koenig, J. M. Kuckelkorn. Neubau der Fach- und Berufsoberschule in Erding: Nachhaltiges Passivhaus mit extreme niedrigem Gesamt-Primaerenergiebedarf: Dokumentation der Bauphase und der Inbetriebnahme. Abschulussbericht, DBU, Osnabrueck, 2014.

[47] Y. Wang, F. Y. Zhao, J. Kuckelkorn etc. Classroom energy efficiency and air environment with displacement natural ventilation in a passive public school building. Energy and Buildings 70 (2014) 258-270.

Figure 1

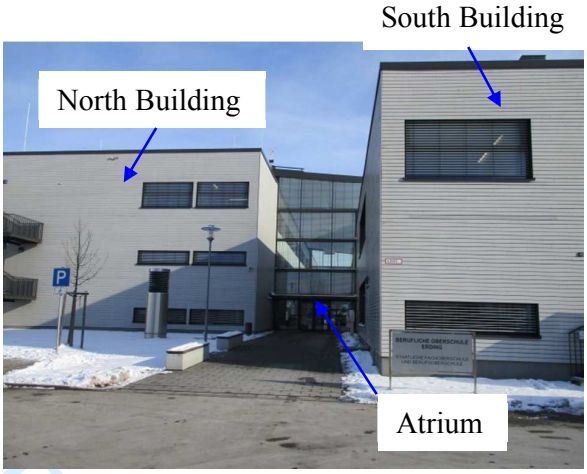

(a) New low-energy school building in Bavaria, Germany

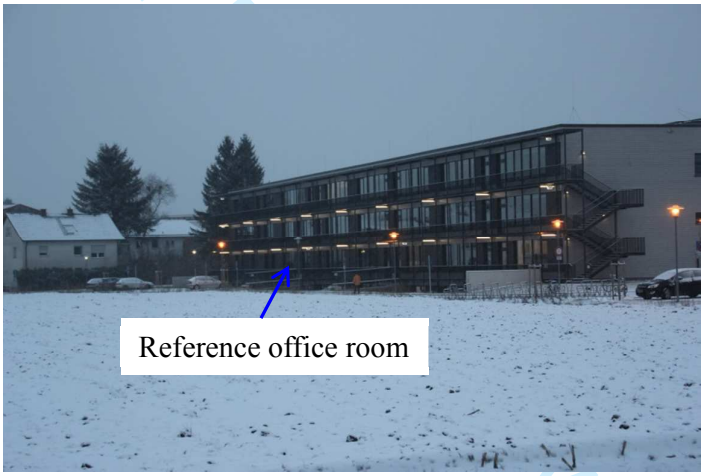

(b) North façade of new low-energy school building and the reference office room

Figure 1: Façade pictures of low-energy building including north and south buildings and atrium (a) and north sides plus the reference office room (b) in winter

Figure 2

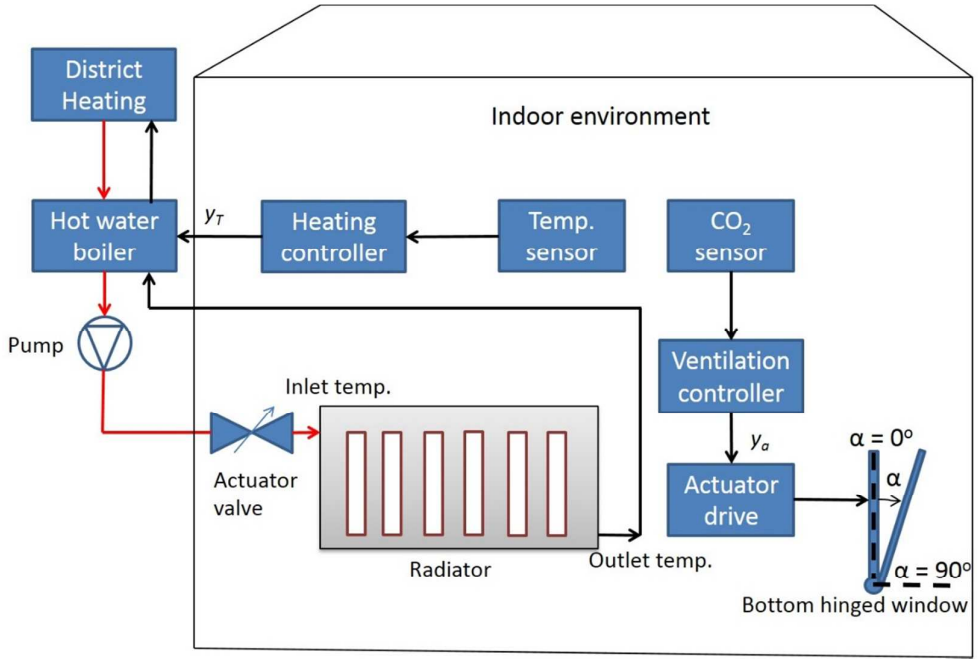

Figure 2: Schematic diagram of the office room with DCV and radiator heating control systems. "y_T" and "y_a" are the output signals of the radiator heating and DCV controllers, respectively, "α" is the opening or tilting angle for the window.

Figure 3

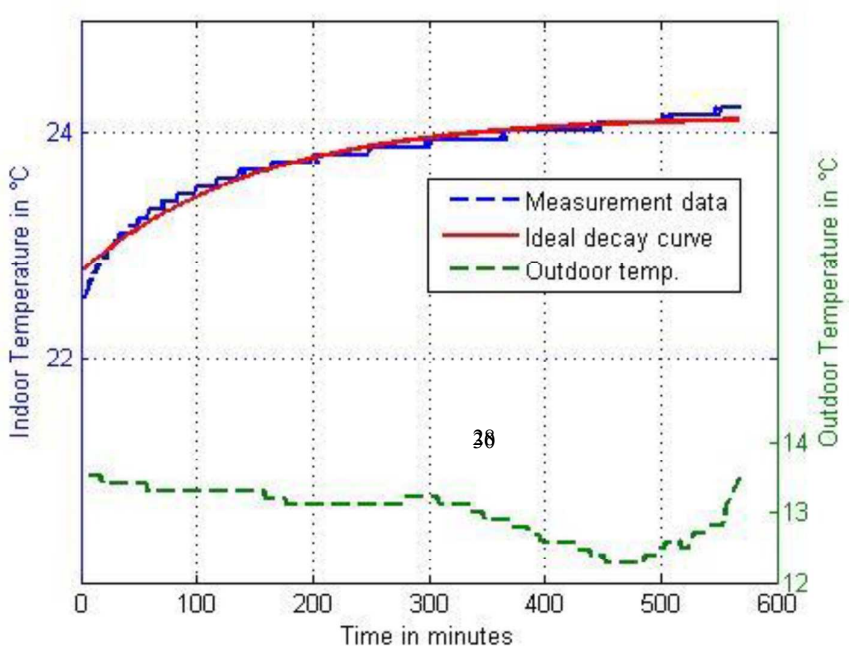

(a)

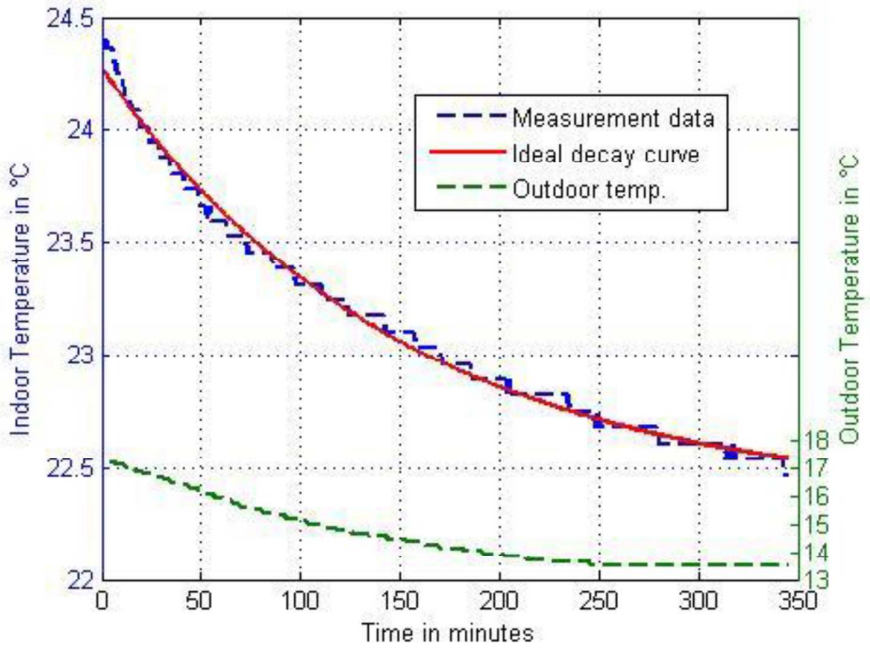

(b)

Figure 3: Indoor air temperature of measurement and regression for calculating thermal time constants for increasing temperatures (a) and decreasing temperatures (b), respectively, in the reference office room, and corresponding outdoor temperatures.

Figure 4

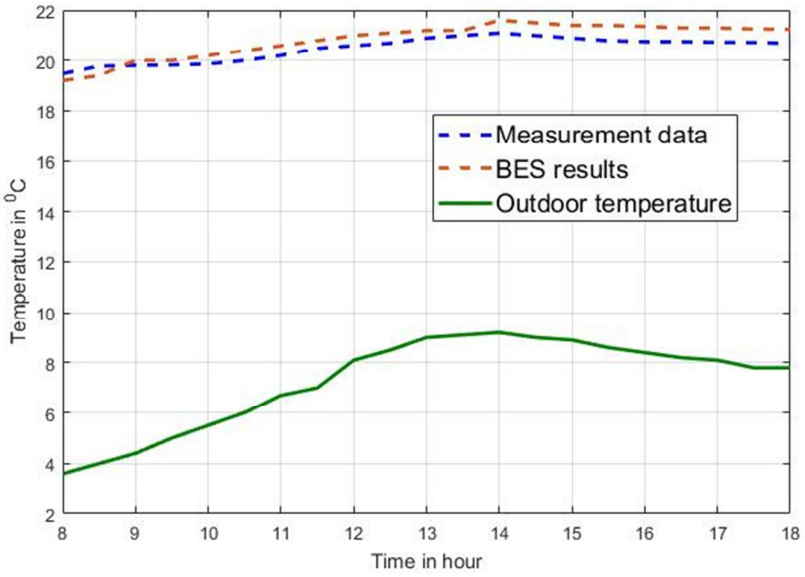
Measurement data
BES results
Outdoor temperature
Temperature in ^{0}C
Time in hour
22
20
18
16
14
12
10
8
6
4
2
8
9
10
11
12
13
14
15
16
17
18

(a)

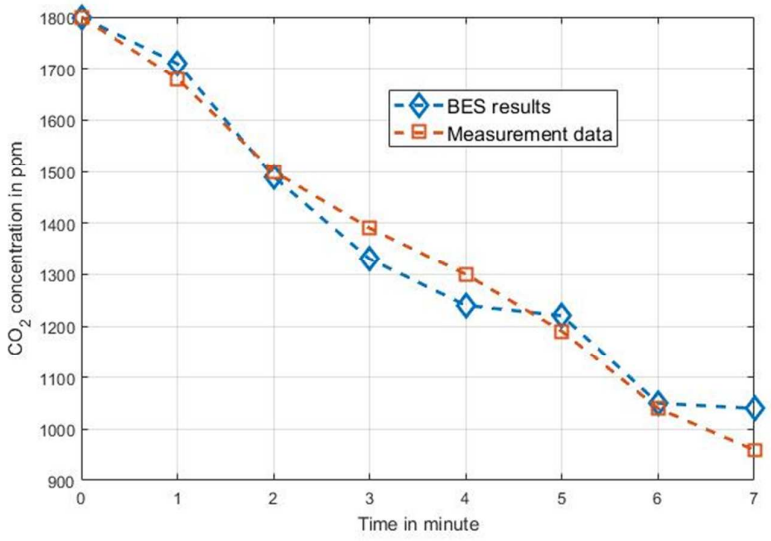

(b)

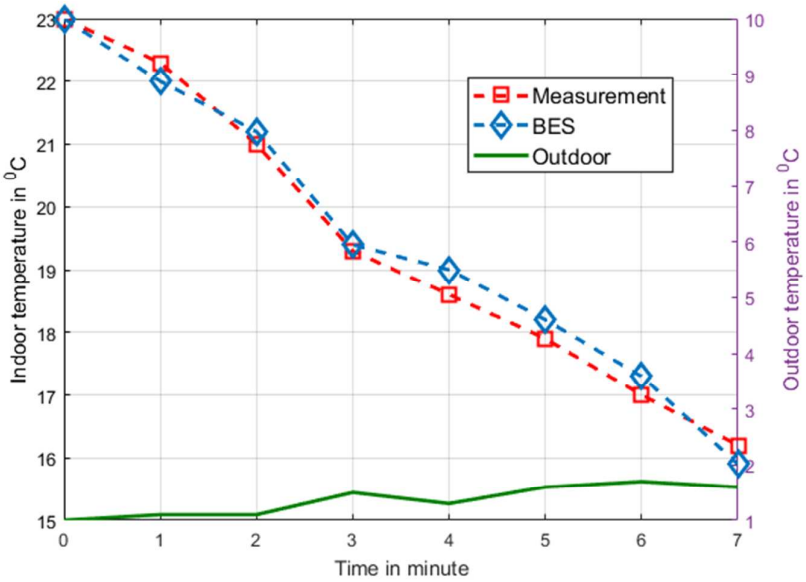

(c)

Figure 4: Indoor temperatures (a) & (c) and CO_2 concentration (b) comparisons of BES and measurements. (a): it demonstrates indoor temperature of BES simulation results (red broken line) and measurement data (blue broken line) in the reference room horizontal coordinate unit is hour, which represents the time of Jan. 5th, 2015. (just with infiltration) (b): it shows indoor CO_2 concentration of BES results (blue diamond line) and measurement data (red square line) under natural ventilation (natural ventilation rate: 3.7 1/h) (c): indoor temperatures of BES simulation results (blue broken line) and measurement data (red broken line) on Nov. 20th, 2014 (outdoor CO_2%: 390 ppm, 30 occupants, mean wind speed: 0.45 m/s, mean wind direction: 270.4^o).

Figure 5

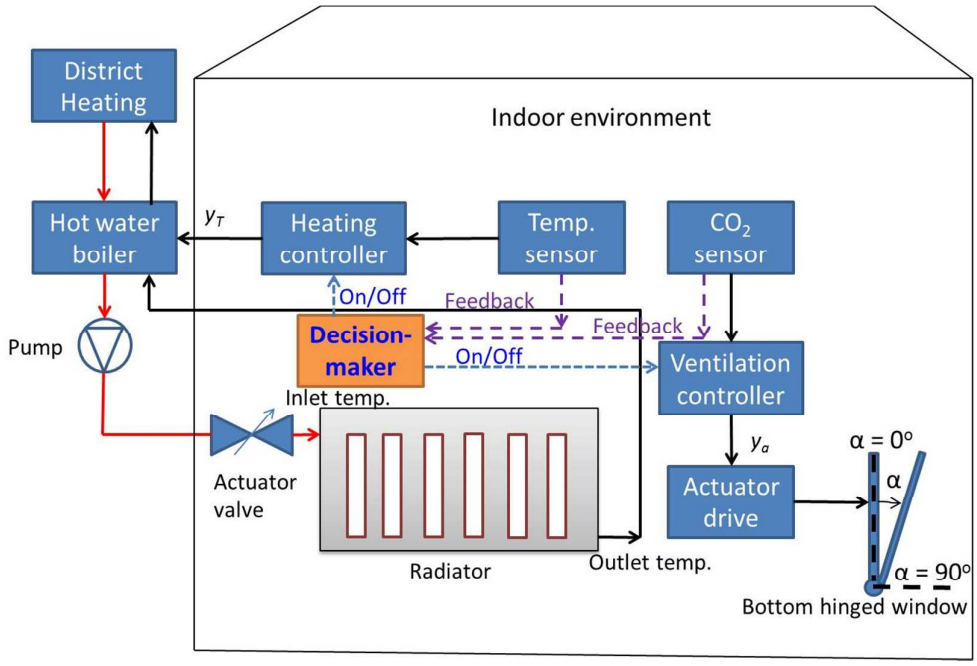

Figure 5: Schematic diagram of the control systems with Decision-maker for coupling DCV and radiator heating.

Figure 6

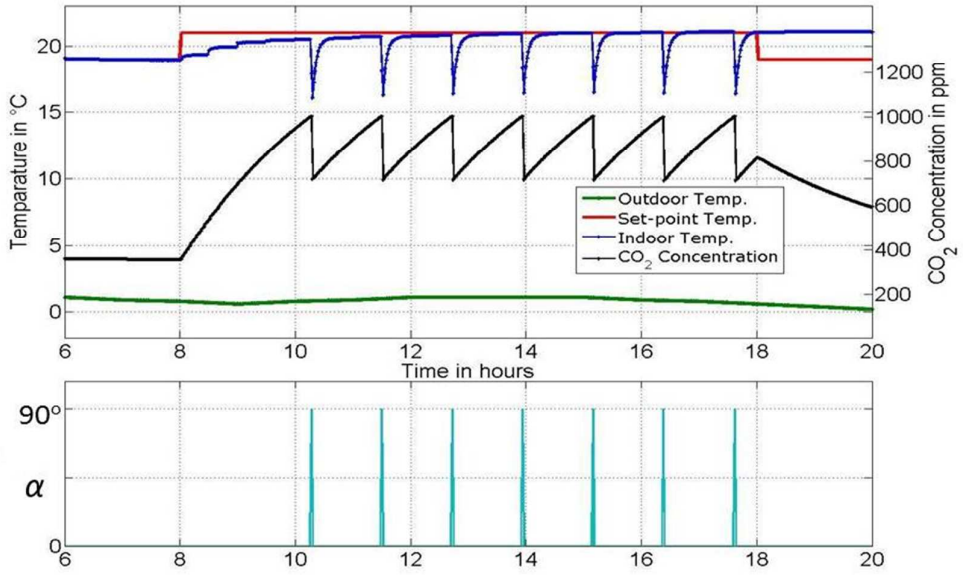

Figure 6: ON/OFF (Bang-bang) ventilation control using $\alpha = 0^o/90^o$ (i.e. OF = 0/1) with an upper set-point for the indoor CO_2 concentration of 1000 ppm. Within the time period of 8 am to 6 pm, windows are opened seven times for one minute causing an obvious decrease of indoor temperature by approximately 5 ^oC (i.e., down to around 16 ^oC). The average CO_2 concentration within the time period between 10:10 am (i.e., first window opening) and 6 pm is 860 ppm (also see Table 3).

Figure 7

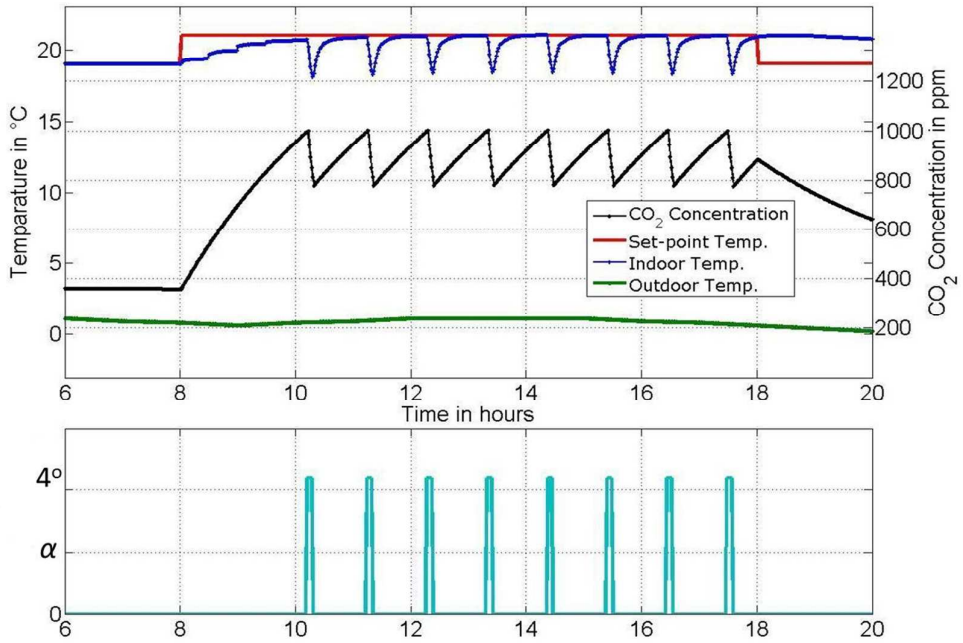

Figure 7: ON/OFF (Bang-bang) ventilation control using $\alpha = 0^{o}/4^{o}$ (i.e., OF = 0/0.04) with an upper set-point for the indoor CO_2 concentration of 1000 ppm. Within the time period of 8 am to 6 pm, both windows are opened eight times for five minutes causing a less obvious decrease of indoor temperature by approximately 3 ^{o}C (i.e., down to around 18 ^{o}C) compared to Figure 6. The average CO_2 concentration within the time period between 10:10 am (first window opening) and 6 pm is still 860 ppm (also see Table 3).

Figure 8

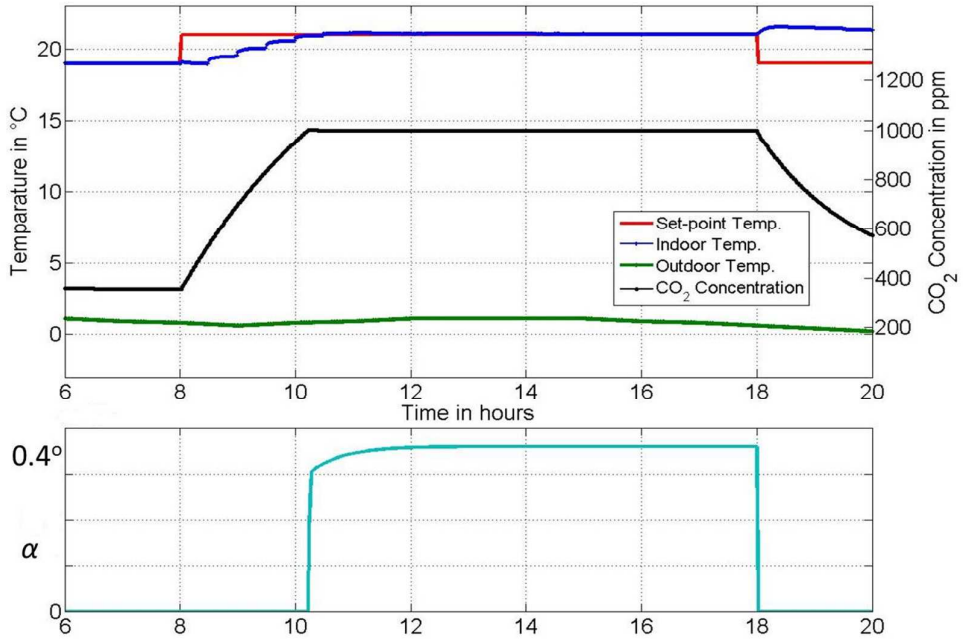

Figure 8: PI(D) control with a set-point for the indoor CO_2 concentration of 1000 ppm. The DCV controller is triggered at 10:10 am when the CO_2 concentration level reaches the set-point for the first time. Within the time period of 10:10 am to 6 pm, both windows are maintained opening with a small $\alpha = 0.4^o$ (i.e. OF = 0.004), which causes a virtually constant indoor temperature of 21 ^oC (i.e., set-point). The average CO_2 concentration within the time period is around 1000 ppm (also see Table 3).

Figure 9

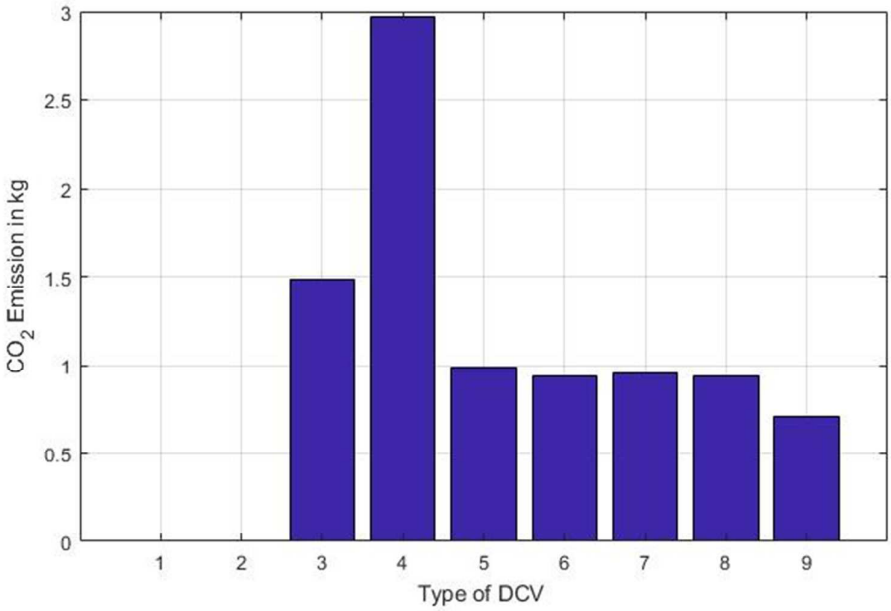

Figure 9: CO_2 equivalent emissions for nine types of DCV corresponding to Q_{air} in Table 3.

Figure 10

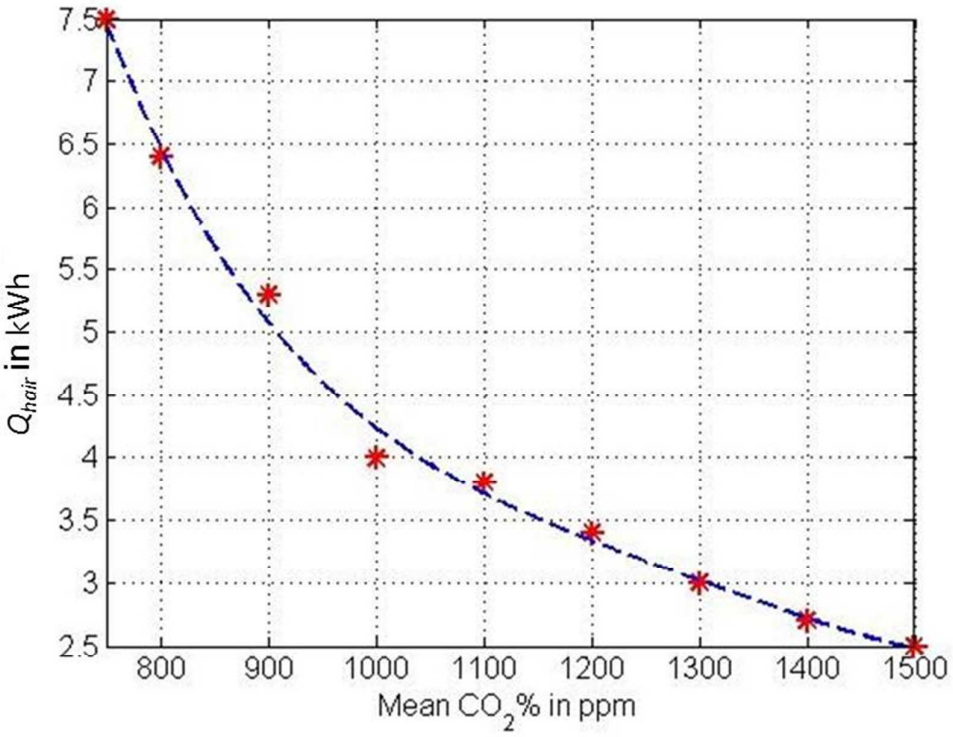

Figure 10: Comparison of Q_{hair} under diverse set points of the CO_2 concentration while using PI(D) control. The values for Q_{hair} were calculated for the average indoor temperature 21 ^{o}C and during the time period from 8 am to 6 pm.

Table 1

Table 1: STD errors for parameters of the exponential decay models

		STD Error
Increasing temperature	T_0	6.342e-3
	k	1.008e-2
	τ	1.232e-4
Decreasing temperature	T_0	1.255e-2
	k	1.048e-2
	τ	1.137e-4

Table 2

Table 2: Combination of coupling control strategies with Decision-maker for ventilation and heating systems

Type	Indoor conditions	Ventilation	Radiator heating	When
No. 1	Not occupied	Off	Off	After working time: night, weekends and holidays
No. 2	Not occupied, but for pre-ventilation and pre-heating	On	On	e.g. one or two hours before work
No. 3	Occupied, just meet the set-points of CO_2%	Off/automatic control mode	On	Working time
No. 4	Occupied, just meet the set-points of indoor temperature	On	Off/automatic control mode	Working time
No. 5	Occupied, but not meet the set-points of CO_2% and indoor temperature	On	On	Working time
No. 6	Occupied, meet the set-points of CO_2% and indoor temperature	Automatic control mode/off	Automatic control mode/off	Working time

Table 3

Table 3 Results for diverse scenarios and ventilation approaches. The values have been calculated for the time period between 10:10 am (i.e., time of first window opening) to 6 pm. All set-point values including temperatures and CO_2 concentration have been determined and employed such that the average values of T_{in} and $CO_2\%$ were virtually the identical to all automated ventilation control methods.

Type	OF_{max}	T_{in} **min max** **°C**	**AVE of** T_{in} **°C**	**STD of the AVE of** T_{in} **°C**	**CO_2% min max ppm**	**AVE of CO_2% ppm**	**STD of the AVE of CO_2% ppm**	Q_{hair} **kWh**
1.Windows closed, no infiltration	0	19.0 21.2	20.9	0.53	390 4390	2380	1160	0
2.Windows closed, with infiltration	0	19.0 21.4	20.9	0.56	390 2290	1597	550	0
3.Manual control (2h/5 min)	1	12.8 21.6	20.7	1.77	390 1180	790	220	8.4
4.Manual control (1h/5 min)	1	12.5 22.1	20.3	2.33	390 770	580	110	16.8
5.ON/OFF control (set point: 1000 ppm)	1	16.4 21.4	21.0	0.94	697 1004	860	86	5.6
6.ON/OFF control (set point: 890 ppm)	0.04	18.2 21.3	21.0	0.70	666 890	860	62	5.3
7.ON/OFF control (set point: 1000/730 ppm)	0.04	18.1 21.7	21.0	0.80	729 1003	860	79	5.4
8.PI(D) control (set point: 860 ppm)	0.005	20.8 21.1	21.0	0.10	856 866	860	2	5.3
9.PI(D) control (set point: 1000 ppm)	0.004	20.9 21.1	21.0	0.10	997 1004	1000	2	4.0

Table 4

Table 4 Q_{tran}, Q_{hair}, Q_{inf} of all nine ventilation approaches shown in Table 3 including typical winter day 1 and 2 for the time intervals from 8 am to 6 pm. All values have been given in kWh with the first number to day time and calculated for the average indoor temperatures and CO_2 concentrations illustrated in Table 3.

Type		**1**	**2**	**3**	**4**	**5**	**6**	**7**	**8**	**9**
Day 1	Q_{tran}	5.6	5.6	5.6	5.6	5.6	5.6	5.6	5.6	5.6
	Q_{hair}	0	0	8.4	16.8	5.6	5.3	5.4	5.3	4.0
	Q_{inf}	0	2.6	2.6	2.6	2.6	2.6	2.6	2.6	2.6
Day 2	Q_{tran}	7.3	7.3	7.3	7.3	7.3	7.3	7.3	7.3	7.3
	Q_{hair}	0	0	10.7	21.4	7.3	6.5	7.2	6.9	5.2
	Q_{inf}	0	3.3	3.3	3.3	3.3	3.3	3.3	3.3	3.3